Colossal elastoresistance and strain-dependent magnetization of phase-separated $(Pr_{1-y}La_y)_{0.7}Ca_{0.3}MnO_3$ thin films

M. C. Dekker, A. D. Rata, K. Boldyreva, S. Oswald, L. Schultz, and K. Dörr
Institute for Metallic Materials, IFW Dresden, Helmholtzstraße 20, 01069 Dresden, Germany
(Received 30 April 2009; revised manuscript received 10 August 2009; published 5 October 2009)

Phase separation into a ferromagnetic (FM) metallic and a charge-ordered (CO) insulating state as found in the manganite $(Pr_{1-y}La_y)_{0.7}Ca_{0.3}MnO_3$ (PLCMO) is expected to be sensitive to structural changes. Reversible biaxial strain has been applied to epitaxially grown films on piezoelectric substrates of $(PbMg_{1/3}Nb_{2/3}O_3)_{0.72}(PbTiO_3)_{0.28}$ (001). Reversible strain experiments give a unique insight into the effect of strain on the magnetization and the electrical resistance, i.e., the so-called elastoresistance, of the films. 100-nm-thick PLCMO films of various Pr/La ratios have been grown using alternating pulsed laser deposition from a La-based and a Pr-based target. We have found a drastic reduction in the resistance, or a "colossal" elastoresistance, upon piezoelectrically controlled release of the tensile strain in the films, characterized by a resistive gauge factor of up to 1800. This result is qualitatively consistent with the magnetic measurements, where a higher saturation magnetization and an increased magnetic transition temperature are observed with the release of tensile strain. The elastoresistance is highest at chemical composition $y \approx 0.6$, the metal-insulator phase boundary, and near the metal-insulator transition temperature, where the competition between the FM and CO ground states is strongest. This indicates that the coexistence of the FM and CO phases is strongly affected by strain with tensile strain suppressing the FM metallic phase.

DOI: 10.1103/PhysRevB.80.144402 PACS number(s): 73.90.+f

I. INTRODUCTION

To denote the response of the electrical resistance of a material to one- or two-dimensional elastic strains, the term elastoresistance has been introduced.[1–4] It is related to the piezoresistance, which describes the change in resistance per applied mechanical stress. Since the 1950s, both properties have been investigated for semiconductors such as doped Si, Ge, and Bi, and have been applied in cantilevers of force microscopes (see, e.g., Refs. 5 and 6). Complex oxides are another class of materials that has shown an outstanding sensitivity of electronic properties to structural deformations. However, not much is known about the piezoresistance and elastoresistance of conducting complex oxides thus far. Earlier work has revealed a large response of the resistance of epitaxially grown ferromagnetic manganite films on a reversibly applied elastic substrate strain.[7–11] Since an even larger effect may be expected in manganites known for the electronically driven coexistence of several phases with different conductivity, the well-investigated compound series of $(Pr_{1-y}La_y)_{0.7}Ca_{0.3}MnO_3$ (Refs. 12–20) has been chosen for a systematic study of the strain-dependent resistance and magnetization in thin epitaxial films. Reversible biaxial strain is applied to the films using piezoelectric substrates.

The end members of the $(Pr_{1-y}La_y)_{0.7}Ca_{0.3}MnO_3$ series are a charge-ordered (CO) antiferromagnetic insulator ($y=0$) and a ferromagnetic (FM) metal ($y=1$), respectively. The nature of the charge-ordered state has been clarified in more detail in recent years; it was found that the idea of a so-called Zener polaron state is more consistent with experimental data than the earlier scheme of a Mn^{3+}/Mn^{4+}-ordered charge lattice.[21] The different effect of the Pr and La ions at the *A* lattice site of the perovskite-type lattice structure is essentially caused by their difference in ionic radius: the smaller Pr^{3+} ion causes a stronger tilt of the O-octahedra and thus smaller Mn-O-Mn bond angles, reducing the width of the conduction band and the itinerant ferromagnetic double exchange. This is the so-called chemical pressure effect. Mixed compounds of $(Pr_{1-y}La_y)_{0.7}Ca_{0.3}MnO_3$ or compounds with a similar doping of $x \approx 0.3$ have been investigated as bulk ceramic phases,[13,14] single crystals,[15] and epitaxially grown films.[17–20] With increasing y, a transition from a CO insulating to a FM metallic state is observed, typically showing a kind of threshold behavior where large changes in conductivity and magnetic transition temperature are observed near a specific composition.[12–14] The long-range CO transition is observed as an anomaly in the resistance vs. temperature data.[19,22] The coexistence of an antiferromagnetic CO and a FM phase has been detected and investigated by neutron scattering,[23] electron diffraction in a transmission electron microscope,[12,21] magnetic force microscopy,[20] and magneto-optical imaging.[15] The extension of the different phases in $(Pr_{1-y}La_y)_{0.7}Ca_{0.3}MnO_3$ may reach the micron range.[12,15,20] Electrical conduction proceeds via percolating conduction paths that can be visualized optically.[24] The metal-insulator (MI) transition, occurring during heating or cooling close to the magnetic Curie temperature (T_C) in the samples with a metallic ground state, has been proposed to be of a percolative nature.[12,25]

The coexistence of the charge-ordered insulating (COI) and ferromagnetic metallic (FMM) phases in PLCMO or related Pr manganites has been found to be sensitive to various external parameters such as electric and magnetic dc fields, light or x rays,[26] hydrostatic pressure,[27] and epitaxial strain in thin films. The most well-known effect of an external parameter is the colossal magnetoresistance, a drop of the electrical resistance by many orders of magnitude under an applied magnetic field. But also an electric field or a current applied to insulating $(Pr_{1-y}La_y)_{0.7}Ca_{0.3}MnO_3$ or $Pr_{1-x}Ca_xMnO_3$ may induce a conducting state,[15,28] i.e., depending on the composition y, electrical conduction may be highly nonlinear. Tokunaga *et al.*[15,16] magneto-optically ob-

served fluctuations of the conduction path depending on the applied electric field, revealing the interaction of a spin-polarized current with the local magnetic state. The response of $Pr_{1-x}Ca_xMnO_3$ to hydrostatic pressure has been found to be rather complex in the sense that the sign of the change in conductivity with pressure depends on the doping level.[27] Uniaxial or biaxial strain studies in bulk materials of the investigated compounds are not known to the authors.

Several groups have investigated thin epitaxial films of phase-separated $(Pr_{1-y}La_y)_{1-x}Ca_xMnO_3$ in the doping range of $x=0.3-0.375$.[17–20,29] Further work on, e.g., $Pr_{1-x}(Ca,Sr)_xMnO_3$ films with $x=0.3-0.4$ (Refs. 28 and 30) shows similar tendencies with respect to T_C and conduction behavior in dependence on composition, since the ionic radius effect is exploited in a similar fashion. The behavior of films that are thick enough not to be dominated by finite thickness effects is subject to one crucial additional parameter: the epitaxial strain in the film plane. It has been shown that the energy balance between the different phases can be controlled by choosing substrates with different lattice mismatch.[17,19,31] As a general tendency, tensile strain is found to stabilize a CO state in several reports.[19,31] Keeping in mind the complex response of $Pr_{1-x}Ca_xMnO_3$ to hydrostatic pressure[27] however, there may be exceptions to this tendency.

By using reversible uniform biaxial strain from piezoelectric $Pb(Mg_{1/3}Nb_{2/3})_{0.72}Ti_{0.28}O_3(001)$ (PMN-PT) substrates,[7,32] we have investigated the direct response of the electrical transport and the magnetization of epitaxial $(Pr_{1-y}La_y)_{0.7}Ca_{0.3}MnO_3$ films to reversible biaxial strain, avoiding any additional influence of variations in composition or microstructure, which may occur when substrates of different lattice mismatch are used. The reversible strain approach is especially useful for studies of transport properties such as the elastoresistance since the comparison of several samples in different strain states may be unreliable due to different microstructures. The composition y has been scanned to find the metal-insulator threshold in the ground state of the strained films which is observed close to $y=0.6$. Films of this composition show a positive elastoresistance characterized by a gauge factor $\Gamma \leq 1800$. The reversible partial release of the as-grown tensile strain in the films leads to an enhanced magnetic Curie temperature (by about 2 K for the strain level of 0.07%), enlarged magnetization and reduced resistance, directly showing the tensile strain to suppress the ferromagnetic double exchange, thus favoring the charge- and orbital-ordered state. The strain dependencies of the magnetization and the resistance are distinctly different from those observed previously in simple ferromagnetic manganite films in that there is a large strain response present far below the Curie temperature.

II. EXPERIMENTAL DETAILS

$(Pr_{1-y}La_y)_{0.7}Ca_{0.3}MnO_3$ films were grown by off-axis pulsed laser deposition (PLD, KrF 248 nm excimer laser) on monocrystalline platelets of PMN-PT(001) from stoichiometric targets of $Pr_{0.7}Ca_{0.3}MnO_3$ (PCMO) and $La_{0.7}Ca_{0.3}MnO_3$ (LCMO). All films have a thickness of 100 nm and were deposited in an oxygen pressure of $p=0.3$ mbar at a substrate temperature of $T=725$ °C with a pulse frequency of $f=2$ Hz.

Films were grown by alternate ablation of the PCMO and LCMO targets with a total number of 30 pulses per one unit-cell layer of grown film. To grow a film with La content y, $30y$ pulses of LCMO and $30(1-y)$ pulses of PCMO were cyclically ablated until the desired thickness was reached. To ensure thorough mixing of the ablated material on the substrate, a 10 s pause was inserted between each 30 pulse cycle. Films have been grown with $y=0$, 0.5, 0.55, 0.57, 0.59, 0.6, 0.63, 0.65, 0.75, and 1. Several samples of nominally the same composition around $y=0.6$ have been grown. Compositions of the films have been analyzed by x-ray photoelectron spectroscopy (XPS) measurements (system PHI 5600 CI, Physical Electronics). The measurements were carried out using nonmonochromatic Kg $K\alpha$ x-ray radiation and 3.5 keV Ar^+ ions (2 mm × 2 mm scan size) for sputtering depth profiling. Atomic concentrations were calculated from the peak intensities using single element sensitivity factors.

The single phase nature, orientation, and lattice structure of the as-grown films have been characterized by $\theta-2\theta$ x-ray diffraction (Siemens D5000, Co $K\alpha$) and, for selected films, by reciprocal space mapping around the (002) and (013) reflections (pseudocubic notation). Atomic force microscopy (AFM, Digital Instruments) has been employed to investigate the film surfaces. Magnetization of the films has been measured in a superconducting quantum interference device magnetometer (Quantum Design). Resistivity measurements in dependence on temperature, magnetic field and reversible substrate strain have been carried out in four-probe geometry in both a superconducting magnet and a cryogen-free refrigerator cryostat. All temperature-dependent data have been recorded during cooling of the sample. A sufficiently low measuring current of $I \leq 10$ μA was chosen so that the films showed Ohmic behavior and no field- or current-induced conductivity variations.

To carry out the strain-dependent measurements, a voltage $V \leq 200$ V was applied along the substrate normal between the PLCMO film on top and a NiCr/Au electrode on the bottom (001) face of the substrate, producing an electric field of $E \leq 6.7$ kV cm^{-1} in the 0.3-mm-thick crystal platelet. The resulting current is lower than 10^{-7} A after the crystal has been poled. The huge resistivity of the substrate ($>10^{10}$ Ω cm) guarantees proper functioning of the manganite film as upper electrode within the measurable range of film resistances. The electric field in the film resulting from the substrate voltage can be estimated as E times the ratio of the resistivities of the film and the substrate. For the measured range of film resistivities, this ratio is below 10^{-8}. The PMN-PT substrate shrinks approximately linearly with increasing E in both in-plane directions.[8] The maximum field of 6.7 kV cm^{-1} leads to 0.07% compression between 300 and 90 K.[8,33] Due to the lack of strain data for PMN-PT below 90 K we evaluate the strain response at low temperatures based on the 90 K strain. Hence, the strain values for $T<90$ K in this work may be systematically overestimated since some strain reduction may occur toward low temperatures. The duration of one field cycle from $E=0$ to 6.7 kV cm^{-1} to 0 was about 15 min.

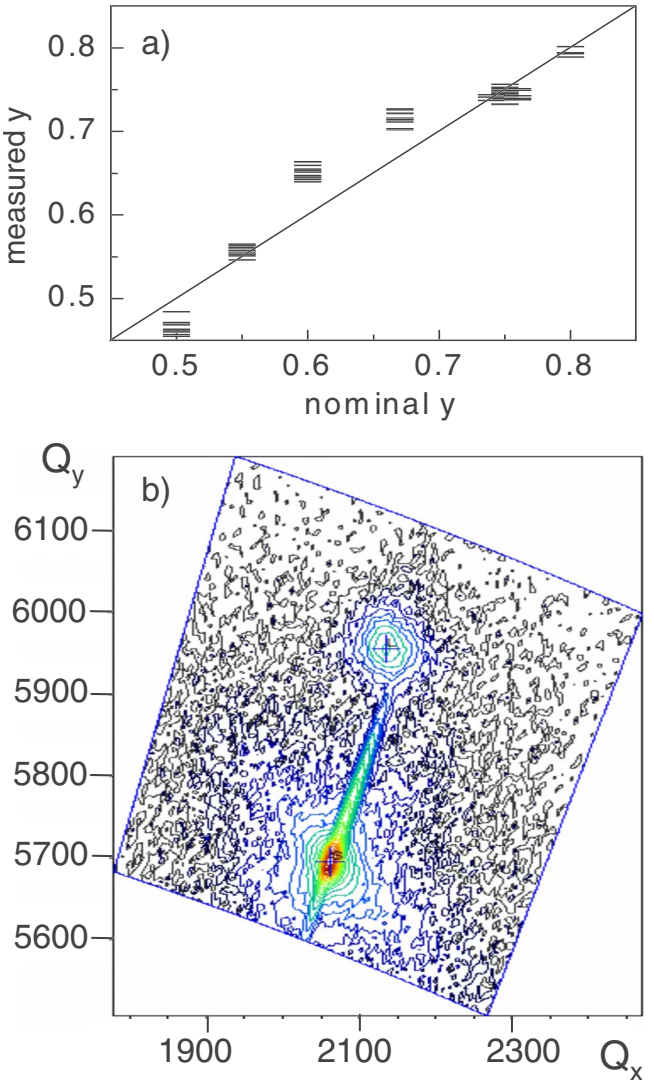

FIG. 1. (Color online) (a) Composition y, determined by XPS, plotted vs. the nominal y, calculated from the number of laser pulses on the respective targets. (Scattering of single data points from various sample depths shown.) (b) X-ray reciprocal space map around the (013) reflection for a $y=0.57$ sample.

III. RESULTS

A. Influence of the composition

X-ray diffraction measurements give evidence that the 100-nm-thick PLCMO films consist of a single chemical phase and are epitaxially oriented in a cube-on-cube way on the substrate [Fig. 1(b)]. AFM images reveal smooth film surfaces grown in the island-type manner with a roughness of rms <1 nm for all films. The roughness has been evaluated within one ferroelectric domain of the substrate, i.e., in a typical area of 1×2 μm^2. The composition of the films has been analyzed by XPS using sputtering depth profiling. In Fig. 1(a), the XPS results of individual runs are compared to the nominal composition of the films for a range of compositions around the metal-insulator phase boundary. The individual data points represent concentration values from several film depths. The agreement between the nominal y calculated from the ratio of the laser pulses on the PCMO and LCMO targets and the value derived from the XPS measurements is within a maximum deviation of 8%. The XPS depth profiles (not shown) did not show concentration gradients with depth, giving evidence for good mixing of the components throughout the film volume. These observations indicate a successful control of the Pr/La ratio of the films by the applied alternating ablation method from two targets.

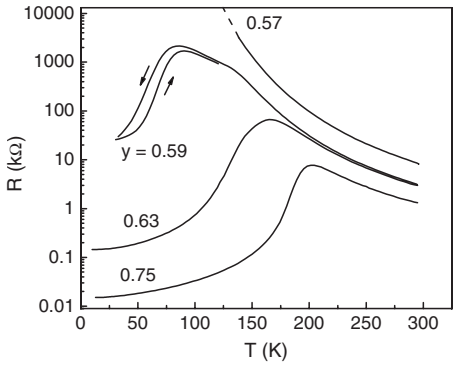

FIG. 2. Electrical resistance of $(Pr_{1-y}La_y)_{0.7}Ca_{0.3}MnO_3$ films as a function of temperature for various values of y. The curves are recorded during cooling. Thermal hysteresis is shown for $y=0.59$.

The pseudotetragonal in-plane lattice parameter of poled PMN-PT crystals is $a=b=4.022$ Å,[33,34] which is 4–5 % larger than the pseudocubic lattice parameters of the end members of the film series, PCMO ($a=3.806$ Å) and LCMO ($a=3.864$ Å). Film lattice parameters have been recorded by reciprocal space mapping for selected samples as $a=3.87$ Å, $c=3.85$ Å for LCMO ($y=1$), $a=3.88$ Å, $c=3.84$ Å for PLCMO ($y=0.6$), and $a=3.84$ Å, $c=3.81$ Å for PCMO ($y=0$). The lattice parameters reveal a residual tensile strain state in the films which are tetragonally distorted with $c/a<1$.

In order to investigate the effect of composition and find the metal-insulator phase boundary, we have prepared films with La concentrations of $y=0$, 0.5, 0.55, 0.57, 0.59, 0.6, 0.63, 0.65, 0.75, and 1. The strained state of the films leads to shifted phase boundaries and transition temperatures with respect to the bulk phase diagram. Figure 2 shows the temperature dependence of the resistance of several films with various y recorded during cooling of the sample. In agreement with earlier studies of both bulk and thin-film samples, a gradual change from the insulating to the metallic ground state is observed with increasing La content, and the metal-insulator transition temperature, T_{MI}, increases with y. A sample is referred to as "insulating" if the resistance is above the measurable range at 10 K. This is done for practical reasons; note that this does not strictly mean the absence of a resistance peak at low temperatures. For compositions below $y=0.59$ the films are insulating at low temperatures (Fig. 2). Close to $y=0.6$, both metallic and insulating samples have been found. Hence, the composition $y=0.6$ represents the metal-insulator phase boundary for our films. Pronounced thermal hysteresis is observed close to this composition (see example in Fig. 2). Magnetic measurements (Fig. 3) prove a systematic increase in the Curie temperature with growing La content. In particular, a steep rise of T_C can be seen

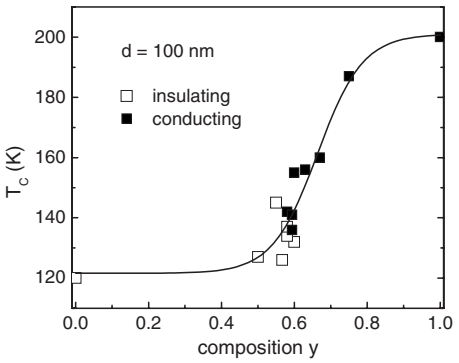

FIG. 3. Magnetic Curie temperature as a function of y. Open and closed symbols indicate samples with insulating and metallic ground states, respectively. The solid line is a guide for the eye.

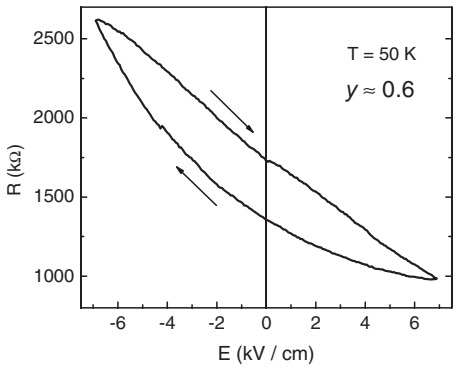

FIG. 4. Resistance of a $y=0.6$ sample as a function of the electric field applied to control the substrate strain. Positive fields result in an in-plane compression, negative fields in expansion of the films.

around the metal-insulator boundary at $y=0.6$ (Fig. 3). Such a relation between T_C and the MI boundary has been noted earlier.[12–14] The T_C of the LCMO end member is suppressed by 50 K with respect to the bulk value. This suppression is essentially attributed to the tensile strain of the film.[8] The T_C of the other end member, PCMO, is reduced by 20 K with respect to the bulk value. Apart from the specific composition at the metal-insulator phase boundary, these observations are in line with the known phase diagram of PLCMO.[12–20] At the metal-insulator transition, percolating electron transport takes place through the FMM clusters, embedded in a COI antiferromagnetic matrix. The low-temperature high-field magnetization M (10 K, 5 T) of the films with $y \leq 0.6$ is reduced to values below 200 emu/cm^3. This is in line with the idea that only a fraction of the film volume is ferromagnetic. A distinct transition to a long-range CO state has not been observed in the films with $y \leq 0.6$ and no distinct antiferromagnetic transition is found in their temperature-dependent magnetization data at any temperature. This is, however, not unusual for films with compositions where the CO state is not very pronounced. Other typical features attributed to the phase coexistence in earlier studies, such as a strong hysteresis in magnetic field dependent resistance data, have been registered (not shown here).

B. Influence of reversible substrate strain

In PLCMO films with $y \approx 0.6$, resistive and magnetic measurements suggest a strong competition between the ferromagnetic metallic and charge-ordered insulating ground states. Therefore, we expect the effect of strain on the balance between the phases to be largest in this region and will focus the study of the reversible strain on these films.

The electrical resistance of our films depends sensitively on the substrate-induced strain. Figure 4 shows a substrate field cycle between +6.7 and −6.7 kV cm^{-1} for a $y=0.6$ film. Note that an approximately linear in-plane expansion occurs for negative field values as long as the ferroelectric coercive field of the substrate is not yet reached.[35] The resistance of the film decreases under biaxial compression ($E>0$) and increases under expansion ($E<0$). It tracks the reversible in-plane substrate strain in an approximately proportional way, but in more detail, the curve is clearly nonlinear and hysteretic. This kind of hysteresis originates from the response of the manganite film to the strain since the strain vs. field characteristic of the substrate itself is not hysteretic beyond the coercive fields.[8] We note that R is not affected by the electric field itself, since this effect should be independent of the sign of E, contrary to the observations such as that in Fig. 4. Summarizing, we find a reduction in the resistance when the as-grown tensile strain of the film is partially released by the piezocompression of the substrate. This effect is seen in all investigated films, regardless of composition. Thus, the samples show a positive elastoresistance and the release of tensile strain acts qualitatively similar to an applied magnetic field, i.e., it enhances the electrical conductivity.

Most strain-dependent measurements have been done in a unipolar manner ($E>0$) to limit the probability of fracture by polarization reversal of the substrate. Figure 5 shows an unipolar measurement at 104 K for a $y=0.6$ sample. The elastoresistance of the film in Fig. 5 is $[R(0)-R(6.7\ \text{kV cm}^{-1})]/R(0)=64\%$. The resistive gauge factor is calculated as $\Gamma=[R(E)-R(0)]/[R(0)\epsilon]$ with the reversible strain $\epsilon=|[a(E)-a(0)]/a(0)|$, and is shown for the same data in the lower panel of Fig. 5. The maximum value of Γ is about 1800, which is an extremely large value for a bulk effect. Recently, a giant room-temperature piezoresistance with $\Gamma=843$ has been observed for an aluminum-silicon hybrid[36] and strained Si nanowires show gauge factors exceeding 1000.[37] Our recent work on strained $La_{0.7}Sr_{0.3}CoO_3$ films revealed an extreme value of Γ near 7000 (Ref. 38) which, however, is not clarified as a bulk effect, but might partially be defect related. Strain-dependent resistance measurements have been taken at various constant temperatures for films with an insulating (Fig. 6) or a metallic (Fig. 7) ground state. The largest elastoresistance is observed in metallic films with $y \approx 0.6$ at temperatures close to the metal-insulator transition temperature. Derived resistive gauge factors are as high as $\Gamma \approx 1000$. Even larger values would be possible depending on the steepness of the $R(T)$ characteristics at T_{MI}.[39] For reasons of (i) the magnitude of the effect being larger, to our knowledge, than published data on bulk elastoresistance of other materials, and (ii) the temperature dependence being similar to that of the colossal magnetoresistance in manganites, we suggest the term "colossal" elas-

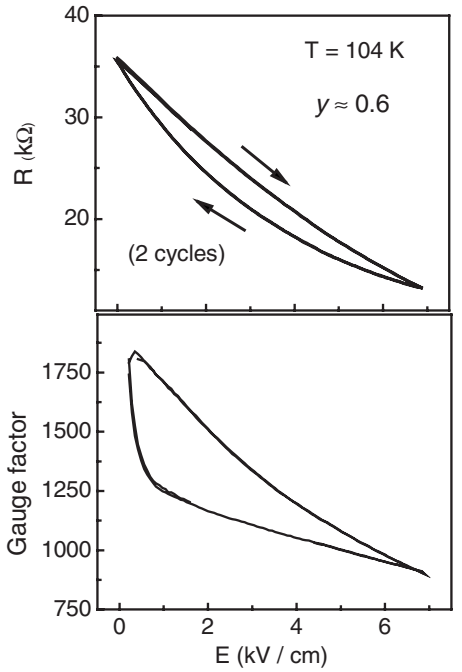

FIG. 5. Upper panel: a unipolar strain-dependent resistance measurement at 104 K for a $y=0.6$ sample. Lower panel: corresponding gauge factor.

toresistance. The elastoresistance observed in the insulating films is much smaller (Fig. 6) with a gradual increase in the gauge factor upon lowering the temperature. Again, we note the qualitative similarity in temperature dependence of the elastoresistance and the magnetoresistance, here for the insulating films. The applied piezocompression was not sufficient to turn an insulating film metallic in the ground state. Contrary to what is known for the magnetoresistance, the elastoresistance does not vanish above the Curie temperature. At 300 K, far above the Curie temperature of the $y=0.6$ samples, still Γ values near 25 are recorded. The elastic deformation of the unit cell also affects high-temperature electrical transport, whereas the field-induced magnetic order becomes negligibly weak far above T_C.

In the following part, the strain dependence of the magnetization is discussed. Figure 8, of a $y=0.6$ film, represents a typical measurement of field-dependent $M(H)$ loops in the

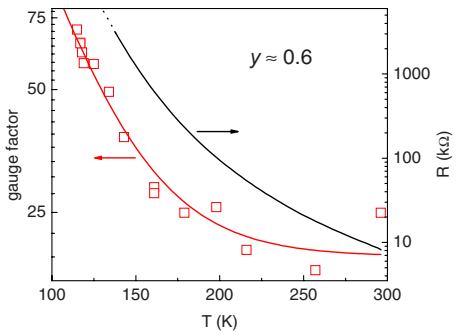

FIG. 6. (Color online) Gauge factor and resistance in dependence on temperature for an insulating sample with composition $y=0.6$.

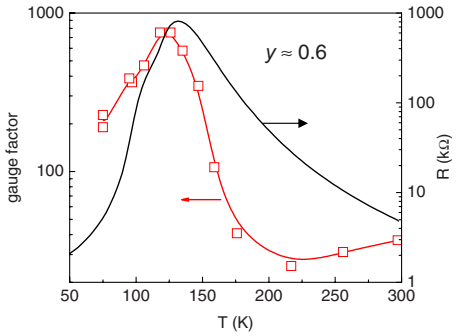

FIG. 7. (Color online) Gauge factor and resistance in dependence on temperature for a metallic film with $y=0.6$.

as-grown and piezostrained state. We note that the commercial NiCr electrode on the PMN-PT backside contributes less than 1% of the saturated signal to the magnetization and shows no strain dependence. Consistent with the transport results, the piezoelectric release of tensile strain leads to an increase in M. The magnetic coercive field remains the same for the applied magnitude of strain (not shown in the figure), indicating a weak effect of the biaxial strain on the magnetocrystalline anisotropy. In contrast, the high-field magnetization is enhanced by more than 10% for the data taken near T_C.[8] (Full saturation is not achieved in fields up to 5 T. Therefore, diamagnetic substrate contribution could not be identified clearly.) For prototypical ferromagnetic manganite films, an extraordinarily large shift of T_C per strain of dT_C/ϵ of up to 190 K/% has been observed.[8] For those films, a strain-dependent T_C underlies the strain-dependent saturated (or spontaneous) M measured at constant temperature. Figure 9 shows $M(T)$ for the as-grown and the piezocompressed state of a $y=0.6$ film. From the $M(T)$ data, a T_C shift of 2 K has been estimated, leading to a value of $dT_C/\epsilon \approx 28$ K/% which is nearly an order of magnitude smaller than the above cited value for a thin $La_{0.7}Sr_{0.3}MnO_3$ film. Similar values have been found for other films with $y \approx 0.6$. Figure 9 also shows the relative change in M between the two strain states, $\Delta M/M(0)$. It peaks slightly above T_C and decreases gradually toward higher as well as lower T. (Note that M in finite fields such as 1 T shows a tail-like decay for $T > T_C$.)

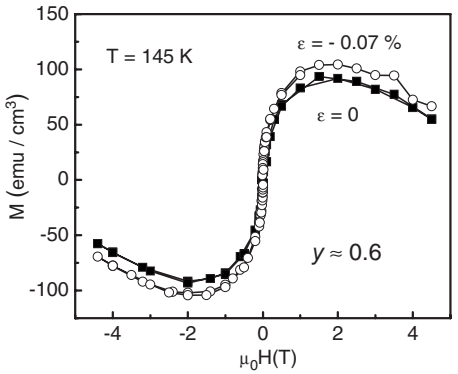

FIG. 8. Magnetization in dependence on applied magnetic field of a sample with $y=0.6$ in the as-grown tensile strained state ($\epsilon=0$) and after piezocompression. The substrate contribution does not depend on strain.

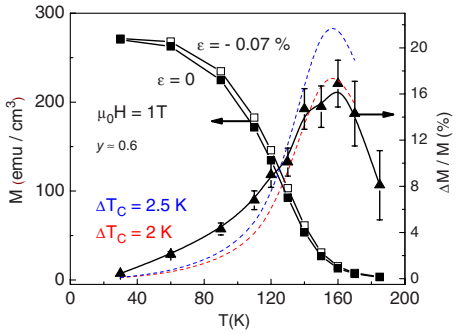

FIG. 9. (Color online) Temperature dependence of the magnetization of a film with $y=0.6$ in two strain states. Also plotted is the relative change in M (closed triangles) and the change in M, estimated for a strain induced T_C shift of 2 and 2.5 K, respectively (dotted lines).

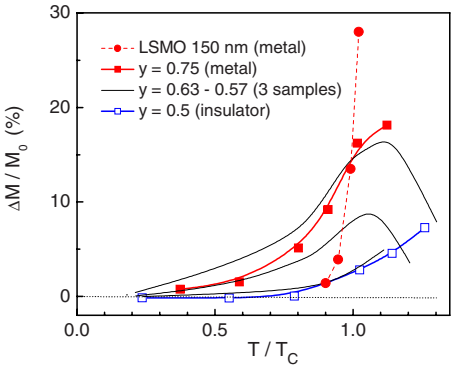

FIG. 10. (Color online) Temperature dependence normalized to T_C of the strain-induced M change in several PLCMO films compared to that of a typical ferromagnetic $La_{0.7}Sr_{0.3}MnO_3$ film.

It is interesting to ask if one can reveal the effect of strain on the phase-separated state in such M data. One may expect to see a strain-dependent M not only close to T_C but also at lower temperatures. For a prototypical ferromagnet with a collinear FM ground state, a shift of T_C is expected to have negligible influence far below T_C. We estimate the pure effect of a strain-dependent T_C shift by approximating the change in M as follows: the $M(T)$ data of the as-grown strain state are shifted with respect to the T axis by ΔT_C, the T_C shift under the piezostrain, and we can calculate the difference $\Delta M^*/M(0)$ between both data sets. If ΔT_C is too small to be measured directly from the $M(T)$ data, it can be adjusted so that $\Delta M^*/M(0)$ fits best to the measured $\Delta M/M(0)$ data around T_C.[35] This approximation, which is sure to overestimate the real effect of a T_C shift at $T \ll T_C$, produced the dashed lines data in Fig. 9 for T_C shifts of 2 and 2.5 K, respectively. These data confirm the directly estimated T_C shift of 2 K. Comparison with the measured $\Delta M/M(0)$ reveals that the actual change in M is more than twice as large as the expected value at temperatures $T<100$ K. This low-temperature behavior differs from the behavior of prototypical ferromagnetic manganites and demonstrates an additional effect of strain on the low-temperature magnetic order. The different temperature dependence of the strain-induced M is also visible in Fig. 10, where the $\Delta M/M(0)$ of several PLCMO films is compared to that of a typical ferromagnetic $La_{0.7}Sr_{0.3}MnO_3$ film. (The behavior of a 150 nm $La_{0.7}Sr_{0.3}MnO_3$ film is expected not to deviate much from a thinner film of the same material.) One notes the more pronounced peak around T_C for the prototypical FM, as well as a more gradual decay toward low T for PLCMO. We suggest that the latter is an effect of the strain on the phase-separated magnetic state of the PLCMO films. In particular, the low-temperature strain response of M reaches a maximum for $y \approx 0.6$ at the metal-insulator phase boundary. It is smaller in the insulating samples with $y=0.5$, a fact tentatively attributed not to the absence of a phase-separated state, but to its lower sensitivity toward the strain. However, it is clear that this low-temperature behavior cannot be explained by assuming a ferromagnetic state with a strain-dependent T_C only.

Magnetization and resistance data in controlled strain states demonstrate a strong suppression of the ferromagnetic double exchange interaction by tensile strain in our films. Piezoelectric release of tensile strain leads to a significant increase in M and a huge reduction in R. The competing CO-AFM state might be additionally favored by tensile strain since it might stabilize the in-plane e_g orbitals. A more detailed mechanism of the effect of strain on a phase-separated FMM/CO-AFM state is difficult to deduce from an investigation of macroscopic properties. It may be speculated that the maximum elastoresistance near the metal-insulator transition is related to the percolative nature of the transport with the release of strain leading to enlarged metallic regions in the sample. In contrast, the smaller strain response of the insulating films reflects the effect of strain on the insulating matrix around FMM clusters.

IV. CONCLUSIONS

In order to investigate the effect of reversible biaxial substrate strain on the properties of the phase-separated PLCMO system, we have prepared films of a range of compositions $y=0-1$ on piezoelectric PMN-PT substrates. The metal-insulator phase boundary has been established to lie at $y \approx 0.6$. Measurements of the magnetization prove a systematic increase in T_C with growing La content. In particular, a steep rise of T_C can be seen around $y=0.6$.

By application of an electric field of $E \leq 6.7$ kV cm^{-1} along the substrate normal, the isotropic in-plane lattice parameter of the PMN-PT substrate is reversibly compressed. The resulting release of tensile strain in the film plane induces a drastic reduction in the resistance, or "colossal" elastoresistance, in films with $y \approx 0.6$. Gauge factors as high as $\Gamma=1800$ have been found around the metal-insulator transition temperature.

Consistent with the transport results, the piezoelectric release of tensile strain leads to an increase in both the ferromagnetic Curie temperature and the magnetization. Compared to prototypical FM manganites, the PLCMO system shows a much more gradual decay of the influence of strain on the magnetization toward low temperatures. This is likely to be an effect of the strain on the magnetic phase coexist-

ence. Both magnetization and resistance data in controlled strain states demonstrate a strong suppression of the ferromagnetic double exchange interaction by tensile strain in the films.

ACKNOWLEDGMENT

Funding of this work by DFG, FOR 520, is gratefully acknowledged.

[1] E. N. Adams, Phys. Rev. **96**, 803 (1954).
[2] J. S. Johannessen, Phys. Status Solidi A **16**, 447 (1973).
[3] R. Koike and H. Kurokawa, Jpn. J. Appl. Phys. **5**, 503 (1966).
[4] S. Onga, W. H. Ko, and Y. Ohmura, J. Appl. Phys. **50**, 7240 (1979).
[5] A. Volodin, D. Buntinx, S. Brems, and C. Van Haesendonck, Rev. Sci. Instrum. **76**, 063705 (2005).
[6] A. Volodin and C. Van Haesendonck, Appl. Phys. A: Mater. Sci. Process. **66**, S305 (1998).
[7] C. Thiele, K. Dörr, S. Fähler, L. Schultz, D. C. Meyer, A. A. Levin, and P. Paufler, Appl. Phys. Lett. **87**, 262502 (2005).
[8] C. Thiele, K. Dörr, O. Bilani, J. Rödel, and L. Schultz, Phys. Rev. B **75**, 054408 (2007).
[9] R. K. Zheng, Y. Jiang, Y. Wang, H. L. W. Chan, C. L. Choy, and H. S. Luo, Appl. Phys. Lett. **93**, 102904 (2008).
[10] K. Dörr, C. Thiele, J.-W. Kim, O. Bilani, K. Nenkov, and L. Schultz, Philos. Mag. Lett. **87**, 269 (2007).
[11] R. B. Gangineni, L. Schultz, C. Thiele, I. Mönch, and K. Dörr, Appl. Phys. Lett. **91**, 122512 (2007).
[12] M. Uehara, S. Mori, C. H. Chen, and S.-W. Cheong, Nature (London) **399**, 560 (1999).
[13] S. H. Masunaga and R. F. Jardim, J. Appl. Phys. **102**, 073903 (2007).
[14] A. M. Balagurov, V. Y. Pomjakushin, D. V. Sheptyakov, N. A. Babushkina, O. Y. Gorbenko, and A. R. Kaul, Physica B (Amsterdam) **350**, 1 (2004).
[15] M. Tokunaga, H. Song, T. Tokunaga, and T. Tamegai, Phys. Rev. Lett. **94**, 157203 (2005).
[16] M. Tokunaga, Y. Tokunaga, and T. Tamegai, Phys. Rev. Lett. **93**, 037203 (2004).
[17] T. Wu, S. B. Ogale, A. Biswas, T. Polletto, R. L. Greene, T. Venkatesan, and A. J. Millis, J. Appl. Phys. **93**, 5507 (2003).
[18] T. Dhakal, J. Tosado, and A. Biswas, Phys. Rev. B **75**, 092404 (2007).
[19] D. Gillaspie, J. X. Ma, H.-Y. Zhai, T. Z. Ward, H. M. Christen, E. W. Plummer, and J. Shen, J. Appl. Phys. **99**, 08S901 (2006).
[20] L. Zhang, C. Israel, A. Biswas, R. L. Greene, and A. de Lozanne, Science **298**, 805 (2002).
[21] L. Wu, R. F. Klie, Y. Zhu, and Ch. Jooss, Phys. Rev. B **76**, 174210 (2007).
[22] Z. Q. Yang, Y. Q. Zhang, J. Aarts, M.-Y. Wu, and H. W. Zandbergen, Appl. Phys. Lett. **88**, 072507 (2006).
[23] H. Sha, F. Ye, P. Dai, J. A. Fernandez-Baca, D. Mesa, J. W. Lynn, Y. Tomioka, Y. Tokura, and J. Zhang, Phys. Rev. B **78**, 052410 (2008).
[24] M. Fiebig, K. Miyano, Y. Tomioka, and Y. Tokura, Science **280**, 1925 (1998).
[25] E. Dagotto, T. Hotta, and A. Moreo, Phys. Rep. **344**, 1 (2001).
[26] V. Kiryukhin, D. Casa, J. P. Hill, B. Keimer, A. Vigliante, Y. Tomokia, and Y. Tokura, Nature (London) **386**, 813 (1997).
[27] C. Cui and T. A. Tyson, Phys. Rev. B **70**, 094409 (2004).
[28] R. C. Budhani, N. K. Pandey, P. Padhan, S. Srivastava, and R. P. S. M. Lobo, Phys. Rev. B **65**, 014429 (2001).
[29] W. Westhäuser, S. Schramm, J. Hoffmann, and C. Jooss, Eur. Phys. J. B **53**, 323 (2006).
[30] N. Takubo, Y. Ogimoto, M. Nakamura, H. Tamaru, M. Izumi, and K. Miyano, Phys. Rev. Lett. **95**, 017404 (2005).
[31] W. Prellier, E. R. Buzin, Ch. Simon, B. Mercey, M. Hervieu, S. de Brion, and G. Chouteau, Phys. Rev. B **66**, 024432 (2002).
[32] O. Bilani-Zeneli, A. D. Rata, A. Herklotz, O. Mieth, L. M. Eng, L. Schultz, M. D. Biegalski, H. M. Christen, and K. Dörr, J. Appl. Phys. **104**, 054108 (2008).
[33] M. D. Biegalski, K. Dörr, D.-H. Kim, and H. M. Christen (unpublished).
[34] A. A. Levin, D. C. Meyer, P. Paufler, C. Thiele, K. Dörr, and L. Schultz, Appl. Phys. A: Mater. Sci. Process. **84**, 37 (2006).
[35] A. Herklotz, A. D. Rata, L. Schultz, and K. Dörr, Phys. Rev. B **79**, 092409 (2009).
[36] A. C. H. Rowe, A. Donoso-Barrera, Ch. Renner, and S. Arscott, Phys. Rev. Lett. **100**, 145501 (2008).
[37] R. He and P. Yang, Nat. Nanotechnol. **1**, 42 (2006).
[38] A. D. Rata, A. Herklotz, K. Nenkov, L. Schultz, and K. Dörr, Phys. Rev. Lett. **100**, 076401 (2008).
[39] A. Biswas (unpublished).